To appear

J. Non Newtonian Fluid Mech

University of Minnesota Supercomputing Institute Research Report UMSI 99/100

UMSI 99/100 May 1999

EFFECTS OF SHEAR THINNING ON MIGRATION OF NEUTRALLY BUOYANT PARTICLES IN PRESSURE DRIVEN FLOW ON NEWTONIAN AND VISCOELASTIC FLUIDS

P.Y. Huang and D.D. Joseph

1200 Washington Avenue South ☐ Minneapolis, Minnesota 55415

Effects of shear thinning on migration of neutrally buoyant particles in pressure driven flow of Newtonian and viscoelastic fluids

by P. Y. Huang and D. D. Joseph

Department of Aerospace Engineering and Mechanics and the Minnesota Supercomputer Institute, University of Minnesota, Minneapolis, MN 55455, USA

January 1999

Abstract. The pattern of cross stream migration of neutrally buoyant particles in a pressure driven flow depends strongly on the properties of the suspending fluid. These migration effects have been studied by direct numerical simulation. Shear thinning has a large effect when the inertia or elasticity is large, but only a small effect when they are small. At moderate Reynolds numbers, shear thinning causes particles to migrate away from the centerline, creating a particle-free zone in the core of the channel, which increases with the amount of shear thinning. In a viscoelastic fluid with shear thinning, particles migrate either toward the centerline or toward the walls, creating an annular particle-free zone at intermediate radii. The simulations also give rise to precise determination of slip velocity distributions in the various cases studied.

---

1. Introduction

Shear thinning is an important property of most polymeric liquids and occurs when the viscosity decreases with increasing intermediate shear rates. This effect can be quite dramatic, with the viscosity decreasing by a factor of up to 10^4.

Boger [1] gave a clear experimental example of low and high shear rate behaviors for a shear thinning (pseudoplastic) fluid. The viscosity of a pseudoplastic fluid decreases with shear rate at intermediate shear rates but is constant at both very low and very high shear rates. Joseph [2] pointed out that the effect of shear thinning is to decrease the viscosity and increase the shear rate at places of constant shear stress. In a viscoelastic fluid, the increased shear rate amplifies the effect of normal stresses at places where the shear stress

is constant. This was confirmed by Huang, Feng, Hu & Joseph [3] in numerical simulations of the motion of a circular cylinder in Couette and Poiseuille flows of an Oldroyd-B fluid. In another study, Garrioch & James [4] performed a computational study of Newtonian and power-law fluids in a conical channel flow. They concluded that shear thinning fluids separate more easily at the junction between the cone and the downstream tube and produce smaller pressure drops than Newtonian fluids. Shear thinning produces both higher velocity gradients and lower viscosities along the wall and therefore reduces the wall shear stresses and experiences smaller viscous pressure drops, but it also causes greater inertial pressure drops across the cone due to the blunter velocity profile. The differences between Newtonian and shear thinning behavior are a combination of viscous and inertial pressure drops. Their numerical simulations showed that shear thinning and Newtonian flows are qualitatively similar but quantitatively very different. Huang, Hu & Joseph [5] found that off-center tilting of ellipses falling in a channel can be stable in shear thinning fluids but is unstable in fluids with constant viscosity.

Pressure driven flow is one of the most common types of channel flow in industry, especially the petroleum and coal industries. If the particles and suspending liquid have different densities, settling or suspending occurs simultaneously with shear-induced migration. The bulk flow also depends on the relative sizes of the buoyancy and shear forces. Morris & Brady [6] performed numerical studies of the influence of particle buoyancy in pressure driven flow of a suspension when inertia is neglected and compared with experimental results. They found that shear induced migration in Stokes flows competes with buoyancy effects, and concluded that the flow behavior depends strongly on both the bulk particle volume fraction and the dimensionless gravitational parameter, but only weakly upon the dimensionless channel width.

Most of the investigations in the literature focus on the effects of shear thinning in Newtonian and generalized Newtonian fluids or the effects of elasticity without shear thinning. Segré & Silberberg [7] reported that in Newtonian fluids, neutrally buoyant

particles migrate into a thin annular region with maximum concentration being at a radial position of about 0.6 of a pipe radius from the centerline. Karnis & Mason [8] studied the migration of spheres in a pipe flow without inertia effects. They observed that neutrally buoyant spheres migrate toward the pipe wall in a purely pseudoplastic fluid but toward the center region of lower shear rate in a viscoelastic fluid with constant viscosity. In contrast, Gauthier, Goldsmith & Mason [9] declaimed that particles migrate toward the region of highest shear rate in very slow flows of pseudoplastic fluids. Then Jefri & Zahed [10] performed an experimental work on the elastic and viscous effects on migration of neutrally buoyant solid spherical particles in plane Poiseuille flow. With low volume solid fraction and creeping flow conditions, they found that the particles are in uniform distribution in a Newtonian fluid but migrate toward the centerline in a non-shear thinning viscoelastic fluid. Recently Tehrani [11] reported an experimental study on the migration of proppant particles in viscoelastic fluids used in hydraulic fracturing. He focused on elastic and shear thinning properties of the suspending fluid and concluded that the flow behavior depends strongly on both the elastic properties and shear rate gradient of the fluids.

Binous & Phillips [12,13] recently performed dynamic simulations of particle motions in viscoelastic fluids. In their method, the suspending fluids were modeled as suspensions of finite-extension-nonlinear-elastic (FENE) dumbbells. In this method, the effects of elasticity are revealed clearly and are consistent with most of the experimental and numerical results shown in literature. But the method is restricted to low Reynolds number and constant shear viscosity. It does not include the effects of inertia and shear thinning. Asmolov [14] studied the inertial lift on a particle in plane Poiseuille flows at large flow Reynolds number but small particle Reynolds number. Using a matched asymptotic expansions method to solve governing equations for a disturbance flow past a particle, he found three major influence factors for the particle migration: channel Reynolds number or the curvature of velocity profile, distance from the wall and slip velocity. There is not much

literature concerned with the isolated and combined effects of inertia, shear thinning and elasticity.

In the present paper we studied the effects of shear thinning on the migration of particles in both Newtonian and viscoelastic fluids. To make the study more precise, we isolated and studied the effects of shear thinning with and without elasticity while keeping the channel width, particle density and size unchanged. We also studied the effect of shear thinning on the volume fraction of solids.

2. Governing equations and numerical methods

Experimental and mathematical analyses and numerical simulations are the major three methods for studying multiphase processes. Experiments give scientists first hand phenomena to study but are sometimes difficult to interpret because competing effects are present. Mathematical analysis can simplify a specific problem and abstract single effects; analysis is always desirable but more often than not is not possible. Here we employ direct numerical simulation which allows us to solve hard problems numerically and to isolate competing effects.

The motion of solid particles satisfies Newton's law:

$$\begin{cases} M\dfrac{dU}{dt} = Mg + F[u] \\ \dfrac{dX}{dt} = U \end{cases} \tag{1}$$

where **M** is the generalized mass matrix of the particle, **X** and **U** are the generalized position and velocity vectors of the particle, **F** is the generalized force vector imposed on the particle by the fluid and **Mg** is gravity. The velocity field $\mathbf{u}(\mathbf{x},t)$ and pressure field $p(\mathbf{x},t)$ in an incompressible fluid is governed by momentum equations:

$$\begin{cases} \nabla \cdot \mathbf{u} = 0 \\ \rho_f \left(\dfrac{\partial \mathbf{u}}{\partial t} + \mathbf{u} \cdot \nabla \mathbf{u}\right) = \rho_f g + \nabla \cdot \sigma \end{cases} \tag{2}$$

where ρ_f is the density of the fluid, **g** is the body force, $\sigma = -p\mathbf{1} + \mathbf{T}$ and **T** is the extra stress tensor. For an Oldroyd-B fluid, the extra stress tensor is given by the constitutive equation:

$$\mathbf{T} + \lambda_1 \overset{\nabla}{\mathbf{T}} = \eta(\mathbf{A} + \lambda_2 \overset{\nabla}{\mathbf{A}}) \tag{3}$$

where $\mathbf{A} = (\nabla\mathbf{u} + \nabla\mathbf{u}^T)$ is the strain-rate tensor; λ_1 and λ_2 are constant relaxation and retardation times; η is the viscosity of the fluid. The fluid reduces to a Newtonian fluid when $\lambda_1 = \lambda_2$ and to an upper convected Maxwell model when $\lambda_1 \neq 0$ and $\lambda_2 = 0$. The no slip condition is exerted on the particle boundaries:

$$\boldsymbol{u} = \boldsymbol{U} + \omega \times \boldsymbol{r} \tag{4}$$

When the fluid is shear thinning, η is a function of the flow shear rate and can be given by the Carreau-Bird viscosity equation:

$$\frac{\eta - \eta_\infty}{\eta_0 - \eta_\infty} = \left[1 + (\lambda_3 \dot{\gamma})^2\right]^{\frac{n-1}{2}} \tag{5}$$

where $\dot{\gamma}$ is the strain-rate defined in terms of the second invariant of the rate strain tensor $\boldsymbol{D} = \frac{1}{2}[\nabla\boldsymbol{u} + (\nabla\boldsymbol{u})^{\mathrm{T}}]$. The power index is n and $0 < n \leq 1$. More details about the equations and numerical computations are given by Huang, Hu & Joseph [5].

3. General conditions for the simulations

With the numerical package we developed, **Particle-Mover**, solid-liquid flow problems can be simulated. Details may be found at the NSF Grand Challenge — KDI/NCC Project Web site:

http://www.aem.umn.edu/Solid-Liquid_Flows/

together with video animations of the cases discussed in this paper.

The computational domain is a 2-D periodic channel of width W=10 cm and length L=21 cm, as shown in figure 1. There are 56 solid particles initially distributed uniformly in the channel (figure 2) and the volume fraction of solids is $C_p = 0.21$. The fluid density is $\rho_f = 1.0\ \mathrm{g \cdot cm^{-3}}$. The particles are neutrally buoyant circular cylinders ($\rho_s = 1.0\ \mathrm{g \cdot cm^{-3}}$)

with diameter d=1 cm and are driven by a pressure gradient dp/dx. In the periodic computation, the particles move out of the domain from the left side and re-enter the domain from the right side. The dimensionless parameters can be defined as:

Reynolds number: $$Re = \frac{\rho_f U a}{\eta}$$

Deborah number: $$De = \frac{\lambda_1 U}{a}$$

elasticity number: $$E = \frac{De}{Re} = \frac{\lambda_1 \eta}{\rho_f a^2}$$

Mach number: $$M = \sqrt{ReDe} = U/\sqrt{\eta/\lambda_1 \rho_f}$$

where U is the maximum velocity of the channel when there are no particles and a is the radius of the particles.

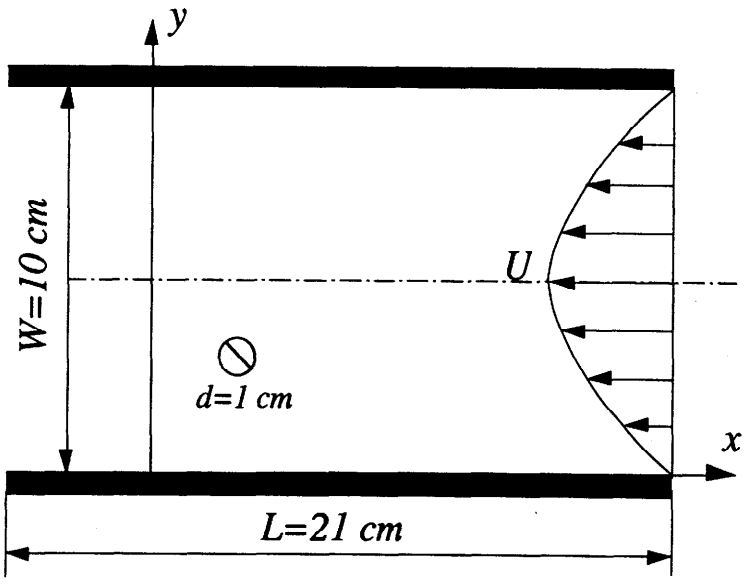

FIGURE 1. Two dimensional periodic domain for computation. W/d=10, L/d=21.

All the computations presented in this paper were carried out using dimensional parameters. A dimensionless description of these results can be constructed by introducing scales: d (which is unit in all of our cases) for length, $\dot{\gamma}_w d$ (shear rate at the wall) for velocity, $1/\dot{\gamma}_w$ for time and $\eta\dot{\gamma}_w$ for stress and pressure.

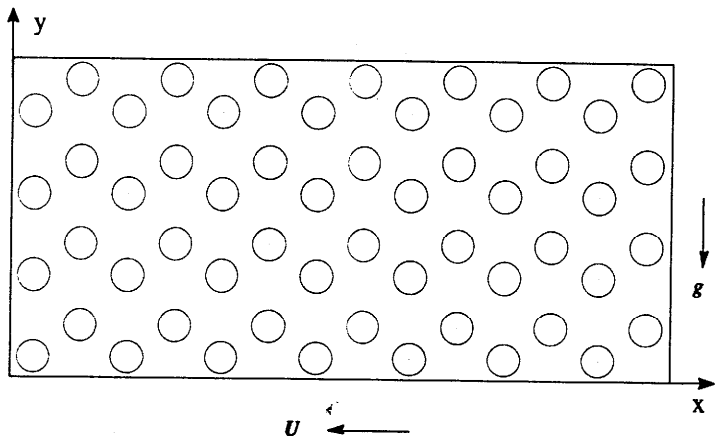

FIGURE 2. Initial positions of the 56 solid particles in a periodic channel. $C_p = 0.21$.

In a Newtonian fluid without shear thinning, the fluid viscosity is constant, the velocity profile of the fully developed flow without particles can be written as:

$$u(y) = -\frac{1}{2\eta}(\frac{dp}{dx})(W - y)y. \tag{6}$$

For a generalized Newtonian fluid, on the other hand, the velocity profile can be implicitly expressed as:

$$\eta\frac{\partial u}{\partial y} = \frac{dp}{dx}(y - \frac{W}{2}) \tag{7}$$

where the fluid viscosity η is a function of the flow shear rate given by equation (5). For a simple shear flow $\dot{\gamma} = \frac{du}{dy}$.

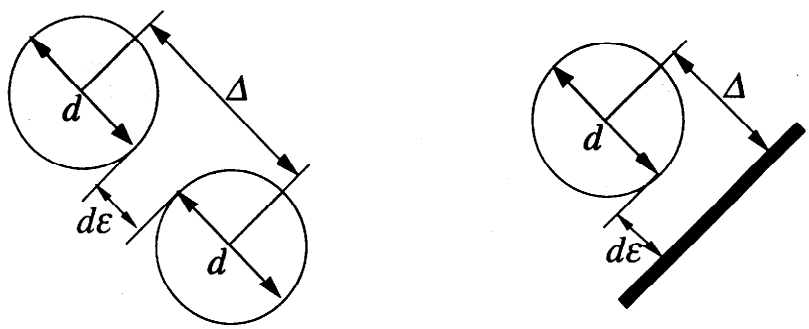

(a) particle-particle (b) particle-wall

FIGURE 3. Detection of collision. The critical distance Δ between two particles or from one particle to a wall satisfies equation (8).

As shown in figure 3, two particles or one particle and a channel wall are said to collide if the distance Δ between the centers of two particles or from the center of one particle to a channel wall is smaller than some critical value given by a relative value ε such that

$$\begin{cases} \Delta \le d(1+\varepsilon) & \text{between two particles,} \\ \Delta \le d(0.5+\varepsilon) & \text{from one particle to a wall.} \end{cases} \tag{8}$$

A specific treatment is used if a collision occurs. We fix ε=5% in all computations carried out for this paper so the smallest distance between two particles is $\Delta_{critical}/d=1.05$ and that from the center of one particle to a channel wall is $\Delta_{critical}/d=0.55$.

4. Results and discussion

As mentioned before, the purpose of this investigation was to study the effects of shear thinning on migration of neutrally buoyant particles in Newtonian and viscoelastic fluids. To isolate the effects of shear thinning, inertia, elasticity and volume fraction of solids, we present the results of our direct numerical simulations in the following four steps: (1) the effects of shear thinning and inertia on migration of particles in Newtonian and generalized Newtonian fluids at moderate Reynolds number are studied; (2) the computations at very small Reynolds number to study the effect of shear thinning without inertial effect; (3) the effects of shear thinning and elasticity on migration of particles in viscoelastic fluids at small Reynolds number; (4) the effect of volume fraction of solids. The numerical results were compared to a series of experimental studies.

4.1. Migration in Newtonian and generalized Newtonian fluids at moderate Reynolds number

Consider the migration of particles in Newtonian and generalized Newtonian fluids with a moderate Reynolds number. The viscosity of the fluid is fixed $\eta = 1.0\ \mathrm{g\cdot cm^{-1}\cdot s^{-1}}$ and the pressure gradient is $|dp/dx| = 2.0\ \mathrm{g\cdot cm^{-2}\cdot s^{-1}}$.

Figure 4 shows the migration of particles in a Newtonian fluid without shear thinning. The maximum fluid velocity is $U_{max} = 25\ \mathrm{cm\cdot s^{-1}}$ at the centerline, which gives the

Reynolds number Re=12.5. The maximum particle velocity is $U_p = 15$ cm·s^{-1} near the centerline and the related maximum slip velocity of the particles $U_{slip} = 10$ cm·s^{-1}, as shown in table 1. The difference of the velocity profile in solid curve and symbols in figure 4(a) is the "slip velocity".

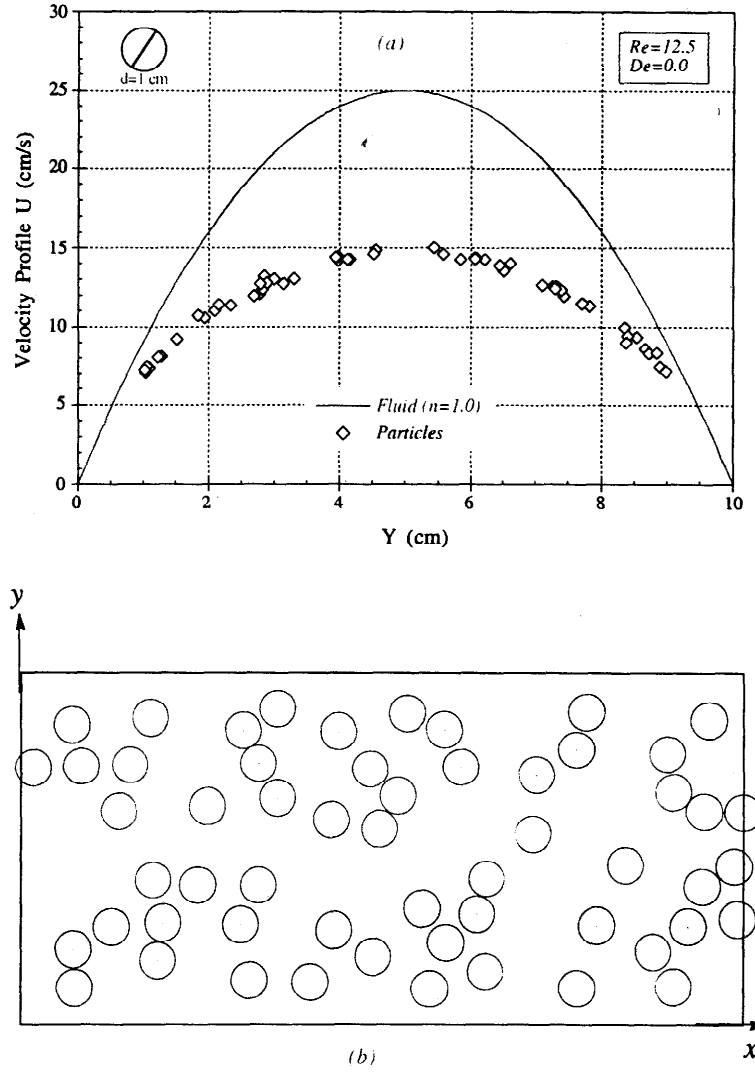

FIGURE 4. Migration of 56 neutrally buoyant particles in a pressure driven flow of a Newtonian fluid without shear thinning (n=1.0). Re=12.5. (a) Velocity profile of the fluid without particles and the velocities of the particles; (b) particle positions in the channel at time t=39.75 s. This flow lubricates in that there are no particles at the center and the particles tend to accumulate at the Segré-Silberberg radius 0.6 (Segré and Silberberg, [7]).

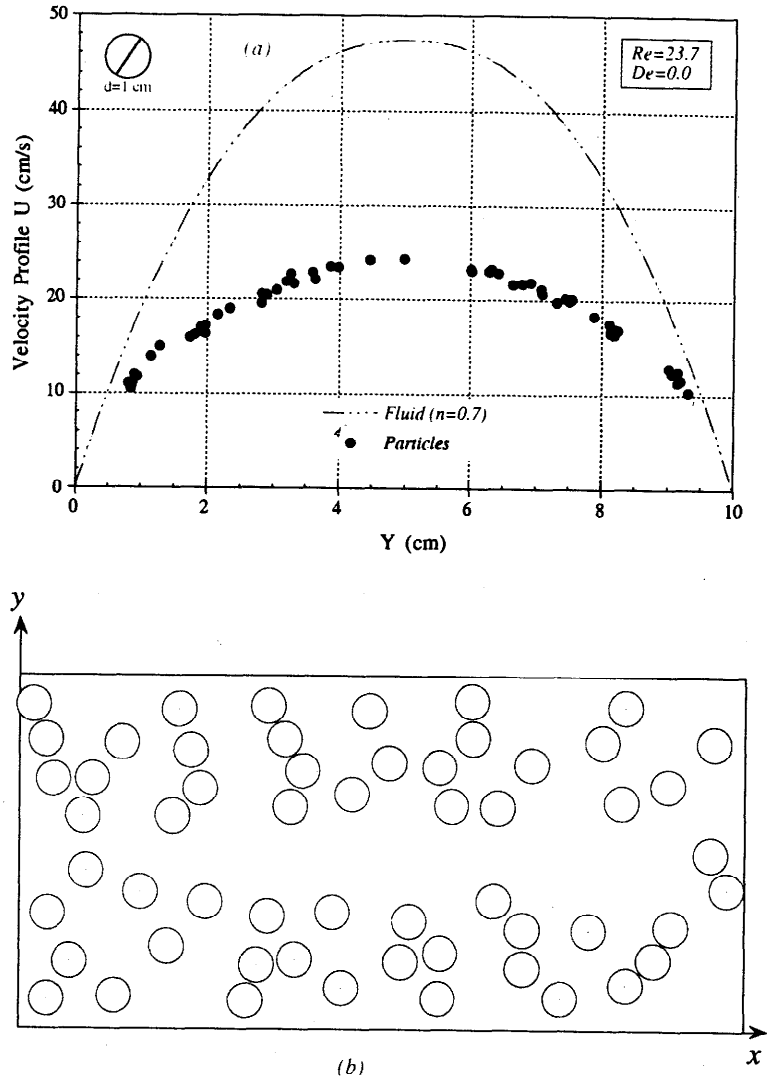

FIGURE 5. Migration of 56 neutrally buoyant particles in a pressure driven flow of a generalized Newtonian fluid (n=0.7). Re=23.7. (a) Velocity profile of the fluid without particles and the velocities of the particles; (b) particle positions in the channel at time t=42.46 s. There is a small "particle-free zone" at the center of the channel.

From figure 4(a), there is a small zone in the center of the channel ($4.550 \le Y \le 5.431$) where there are no particles. The size of this "particle-free zone" is $\Delta_{zone}=0.881$ for n=1.0. Also there are no particles near the channel walls ($Y \le 1.035$ and $Y \ge 8.997$). The average gap between the center of the particles and the channel wall is $\Delta_{gap}=1.019$. The particles are located between $1.035 \le Y \le 4.550$ and $5.431 \le Y \le 8.997$, as shown in table 2.

Lubrication forces move the particles away from the channel walls while the curvature of the velocity profile moves the particles away from the centerline of the channel where the shear rate is zero. This case has been computed for 400 time steps until time t=39.75 second. The particle positions at this time is shown in figure 4(b).

n	Re	U_{max}	U_p	U_{slip}
1.0	12.5	25	15	10
0.7	23.7	47.4	24.4	23
0.5	42.3	84.5	29.6	54
0.4	56.0	111.9	30.5	81.4

TABLE 1. The maximum slip velocity of the neutrally buoyant particles in a pressure driven flow of generalized Newtonian fluids. U_{slip} increases rapidly when the effects of shear thinning become larger (n smaller). All velocities are expressed in $cm \cdot s^{-1}$.

Now consider a generalized Newtonian fluid. With the Carreau-Bird viscosity law, the effects of shear thinning can be imposed by decreasing the power index in equation (5). To isolate the effects of shear thinning, we keep all the other parameters the same as in the Newtonian fluid (n=1.0). The parameters used in this case are: $\eta_0 = 1.0\ g \cdot cm^{-1} \cdot s^{-1}$, $\eta_\infty / \eta_0 = 0.1$, and $\lambda_3 = 1.0\ s$.

n	Re	Y_{min}	Y_1	Y_2	Y_{max}	Δ_{zone}	Δ_{gap}
1.0	12.5	1.0350	4.550	5.431	8.997	0.881	1.0190
0.7	23.7	0.7986	3.981	6.006	9.305	2.025	0.7468
0.5	42.3	0.6428	3.796	5.918	9.264	2.122	0.6894
0.4	56.0	0.6517	3.805	6.211	9.326	2.406	0.6629

TABLE 2. The particle-free zone Δ_{zone} and the average gap Δ_{gap} between the center of the particles and the channel walls in the migration of 56 neutrally buoyant particles in a pressure driven flow of generalized Newtonian fluids. When the effects of shear thinning increase, the particle-free zone (Y_1, Y_2) becomes larger and the particles move closer to the channel walls. The Y's and Δ's are in centimeters.

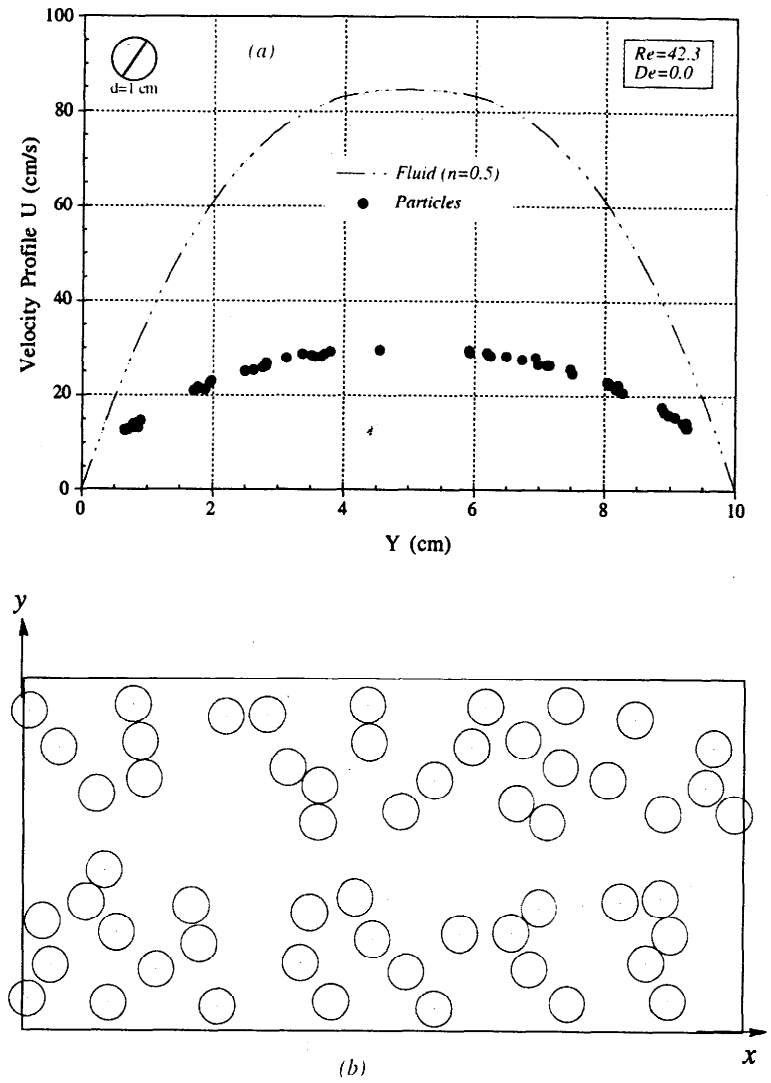

FIGURE 6. Migration of 56 neutrally buoyant particles in a pressure driven flow of a generalized Newtonian fluid (n=0.5). Re=42.3. (a) Velocity profile of the fluid without particles and the velocities of the particles; (b) particle positions in the channel at time t=31.78 s. The particles migrate toward the wall.

The velocity profile with shear thinning is much different from that of n=1.0. From table 1 for n=0.7, the maximum fluid velocity at the centerline is $U_{max} = 47.4\ \text{cm}\cdot\text{s}^{-1}$ and the Reynolds number is Re=23.7. The maximum particle velocity is $U_p = 24.4\ \text{cm}\cdot\text{s}^{-1}$. Now the maximum slip velocity $U_{slip} = 23\ \text{cm}\cdot\text{s}^{-1}$ is much larger than that in a Newtonian fluid without shear thinning (n=1.0). The stresses induced by shear thinning move the particles away from the centerline of the channel, as shown in figure 5(a) where the

"particle-free zone" near the centerline ($3.981 \le Y \le 6.006$) becomes much larger ($\Delta_{zone}=2.025$). The few particles in the center would migrate away in a longer simulation. The particles migrate to the channel wall, the gap becomes much smaller ($\Delta_{gap}=0.7468$). From table 2, the particles finally located between $0.7986 \le Y \le 3.981$ and $6.006 \le Y \le 9.305$. The computations for this case has been carried out to t=42.46 second; the particle positions at this time is shown in figure 5(b).

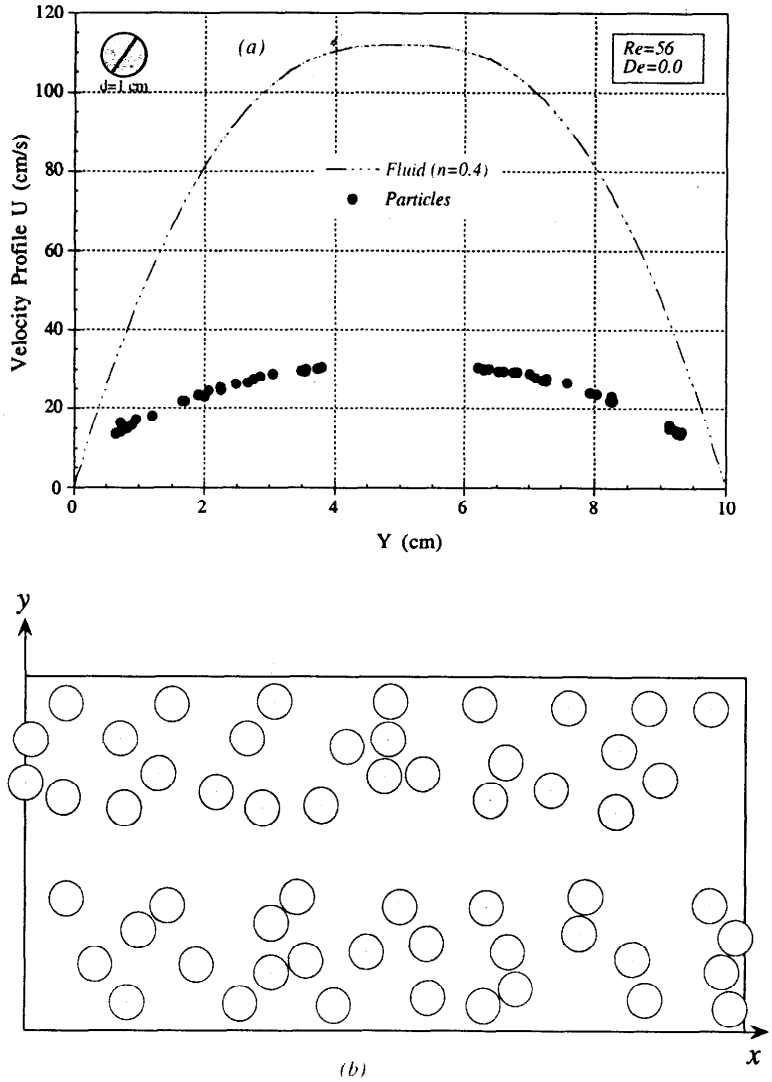

FIGURE 7. Migration of 56 neutrally buoyant particles in a pressure driven flow of a generalized Newtonian fluid (n=0.4). Re=56. (a) Velocity profile of the fluid without particles and the velocities of the particles; (b) particle positions in the channel at time t=25.66 s.

To increase the effect of shear thinning, we reduce the power index to n=0.5; the maximum fluid velocity is $U_{max} = 84.5$ cm·s^{-1} at the centerline and Re=42.3. The maximum particle velocity is $U_p = 29.6$ cm·s^{-1}. Now the maximum slip velocity of the particles is as high as $U_{slip} = 54$ cm·s^{-1}. As shown in figure 6(a), the strong stresses induced by shear thinning move the particles away from the centerline of the channel, the "particle-free zone" near the centerline (Δ_{zone}=2.122) is a little larger than that for n=0.7. There is still one particle in this zone at the time shown in figure 6 and this particle would migrate away from the zone. The particles also migrate much closer to the channel wall (Δ_{gap}=0.6894) and locate between 0.6428≤Y≤3.796 and 5.918≤Y≤9.264. The particle positions at time t=31.78 second is shown in figure 6(b).

n	Re	Y_{min}	Y_1	Y_2	Y_{max}	Δ_{zone}	Δ_{gap}
1.0	12.500	1.0350	4.550	5.431	8.997	0.881	1.0190
1.0	2.500	0.5942	——	——	9.450	——	0.5721
1.0	0.156	0.5516	——	——	9.450	——	0.5508
1.0	0.000	0.6134	——	——	9.420	——	0.5967
0.5	42.300	0.6428	3.796	5.918	9.264	2.122	0.6894
0.5	4.940	0.8231	4.443	5.526	9.266	1.083	0.7786
0.5	0.157	0.5499	——	——	9.450	——	0.5500
0.5	0.000	0.5500	——	——	9.450	——	0.5500

TABLE 3. The particle-free zone Δ_{zone} and the average gap Δ_{gap} between the particles and the channel walls. in the migration of 56 neutrally buoyant particles in a pressure driven flow of a generalized Newtonian fluid. When the effects of shear thinning increase, the particle-free zone (Y_1, Y_2) becomes larger and the particles move closer to the channel walls. All lengths are in centimeters.

We increase shear thinning by reducing the power index to n=0.4; this is the smallest index we can run with our **Particle-Mover** package. The Reynolds number increases rapidly to Re=56 with only modest increase of the maximum particle velocity to $U_p = 30.5$ cm·s^{-1}. From figure 7(a) and table 1, we can see that the maximum slip velocity of the particles for n=0.4 is $U_{slip} = 81.4$ cm·s^{-1}, which is the largest slip velocity for all cases presented in this section. All the particles migrate away from the "particle-free zone"

($3.805 \le Y \le 6.211$) in the centerline and close to the channel wall. The size of the particle-free zone ($\Delta_{zone}=2.406$) reaches its maximum while the gap between the particles and the channel walls ($\Delta_{gap}=0.6629$) has the smallest value. The particles locate between $0.6517 \le Y \le 3.805$ and $6.211 \le Y \le 9.326$ at time $t=27.41$, as shown in figure 7(b).

We can conclude from figures 4-7 and table 2 that in a pressure driven flow of neutrally buoyant particles the effects of shear thinning and the curvature of the velocity profile induce strong shear stresses and large slip velocities, thereby causing the particles to migrate away from the centerline of the channel and move toward the channel walls.

The flow behavior is consistent with the experimental results by Segré & Silberberg [7], Tehrani [11] and the calculations by Asmolov [14]. Tehrani observed the migration of proppant particles in either uncrosslinked or lower crosslinked fluids at low flow rates and found that the particles migrate toward the pipe walls. In his experiment, the fluids have very low normal stresses at low flow rates, therefore, can be treated as Newtonian or generalized Newtonian fluids. Asmolov [14] declaimed that the inertial lift on a spherical particle strongly depends on the curvature of the velocity profile, the distance from the wall and the slip velocity.

4.2. Migration in Newtonian and generalized Newtonian fluids at smaller Reynolds number

To focus our attention on the effects of shear thinning and reduce the effects of inertia, we compute similar cases with smaller Reynolds numbers.

In figures 8 and 9, the pressure gradient is reduced to $|dp/dx| = 0.5\ \mathrm{g\cdot cm^{-2}\cdot s^{-1}}$ and all the other parameters are the same as in section 4.1. Without shear thinning ($n=1.0$), the Reynolds number is $Re=2.5$ and the slip velocity of the particles is $U_{slip} = 2.53\ \mathrm{cm\cdot s^{-1}}$. The particles migrate toward the centerline, there is no "particle-free zone" in the channel. The particles also migrate toward the channel walls, the gap from the particles to the walls ($\Delta_{gap}=0.5721$) is very small, as shown in table 3. The effect of inertia is too small to migrate the particles away from the center and the channel walls.

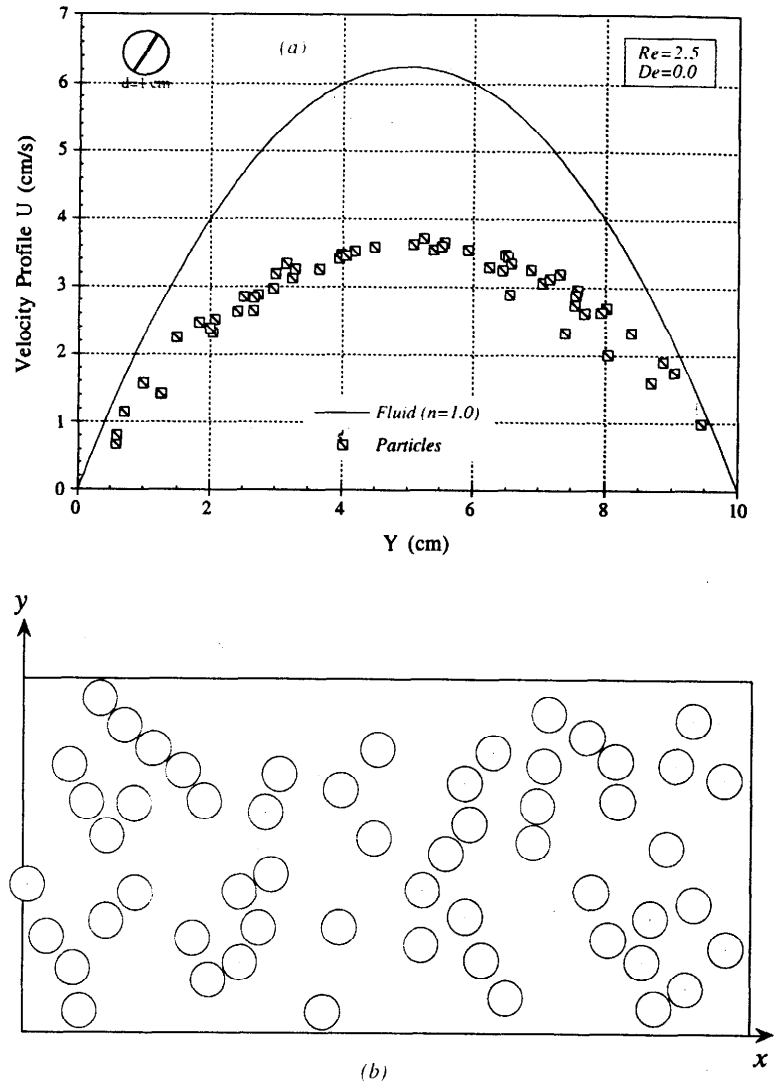

FIGURE 8. Migration of 56 neutrally buoyant particles in a pressure driven flow of a Newtonian fluid without shear thinning (n=1.0). Re=2.5. (a) Velocity profile of the fluid without particles and the velocities of the particles; (b) particle positions in the channel at time t=248.1 s. There is no "particle-free zone" in the center.

When the shear thinning index n=0.5, the Reynolds number is Re=4.94 and the slip velocity is $U_{slip} = 4.19\ \text{cm}\cdot\text{s}^{-1}$. A "particle-free zone" develops at the centerline (Δ_{zone}=1.083, see figure 9), although it is smaller than the one with n=0.5 and Re=42.3 (Δ_{zone}=2.122; there is also a small gap between the particles and the channel walls

(Δ_{gap}=0.7786). The stresses induced by shear thinning are large enough to move the particles away from the centerline and from the channel walls.

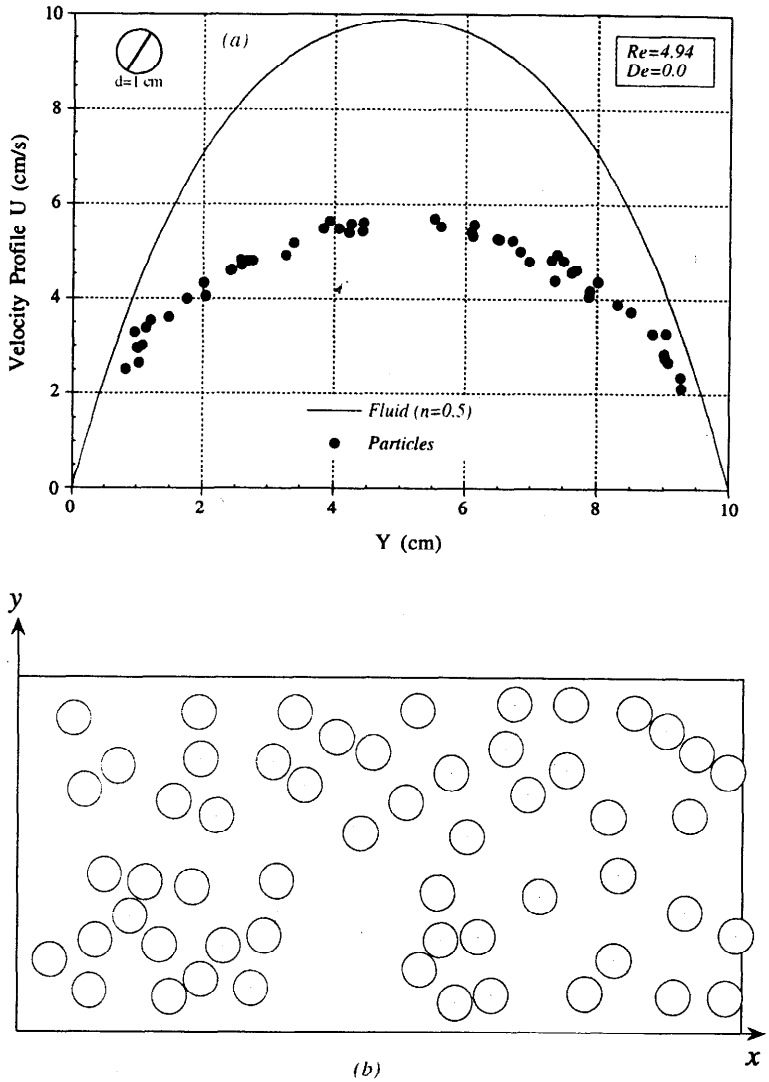

FIGURE 9. Migration of 56 neutrally buoyant particles in a pressure driven flow of a generalized Newtonian fluid (n=0.5). Re=4.94. (a) Velocity profile of the fluid without particles and the velocities of the particles; (b) particle positions in the channel at time t=91.87 s. A small "particle-free zone" develops at the center.

Now we reduce the pressure gradient to $|dp/dx| = 0.1\ \mathrm{g\cdot cm^{-2}\cdot s^{-1}}$ and change the fluid viscosity to $\eta_0 = 2.0\ \mathrm{g\cdot cm^{-1}\cdot s^{-1}}$ while all the other parameters are the same as in section 4.1. The results are shown in figures 10 and 11.

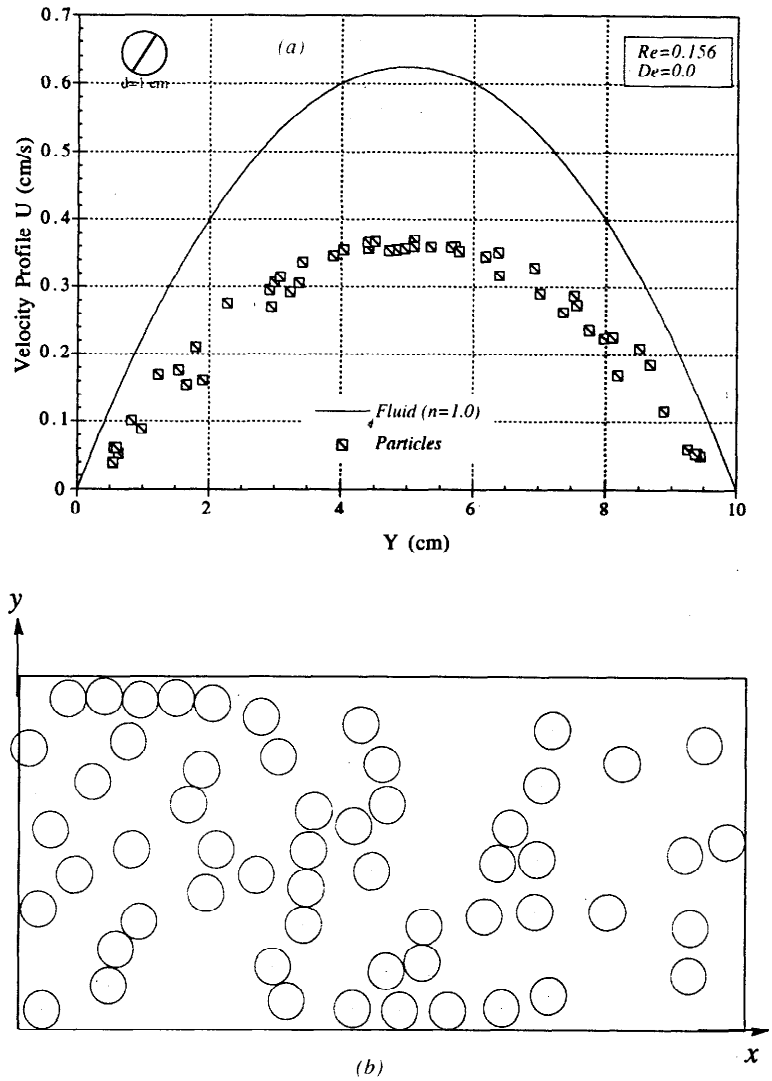

FIGURE 10. Migration of 56 neutrally buoyant particles in a pressure driven flow of a Newtonian fluid without shear thinning (n=1.0). Re=0.156. (a) Velocity profile of the fluid without particles and the velocities of the particles; (b) particle positions in the channel at time t=2728.8 s. There is no "particle-free zone" at the center. Segré-Silberberg effects have not yet taken hold because inertial forces are weak and the simulation time is not very long.

Without shear thinning (n=1.0), the Reynolds number is Re=0.156 and the maximum slip velocity of the particles is $U_{slip} = 0.255\ \text{cm}\cdot\text{s}^{-1}$. For n=0.5, the Reynolds number is Re=0.157 and the maximum slip velocity of the particles is $U_{slip} = 0.269\ \text{cm}\cdot\text{s}^{-1}$. Figures 10 and 11 show that there is no "particle-free zone" in the center for both cases. The effect

of inertia is not strong enough to move the particles away from the centerline, even with the help of the stresses induced by the shear thinning.

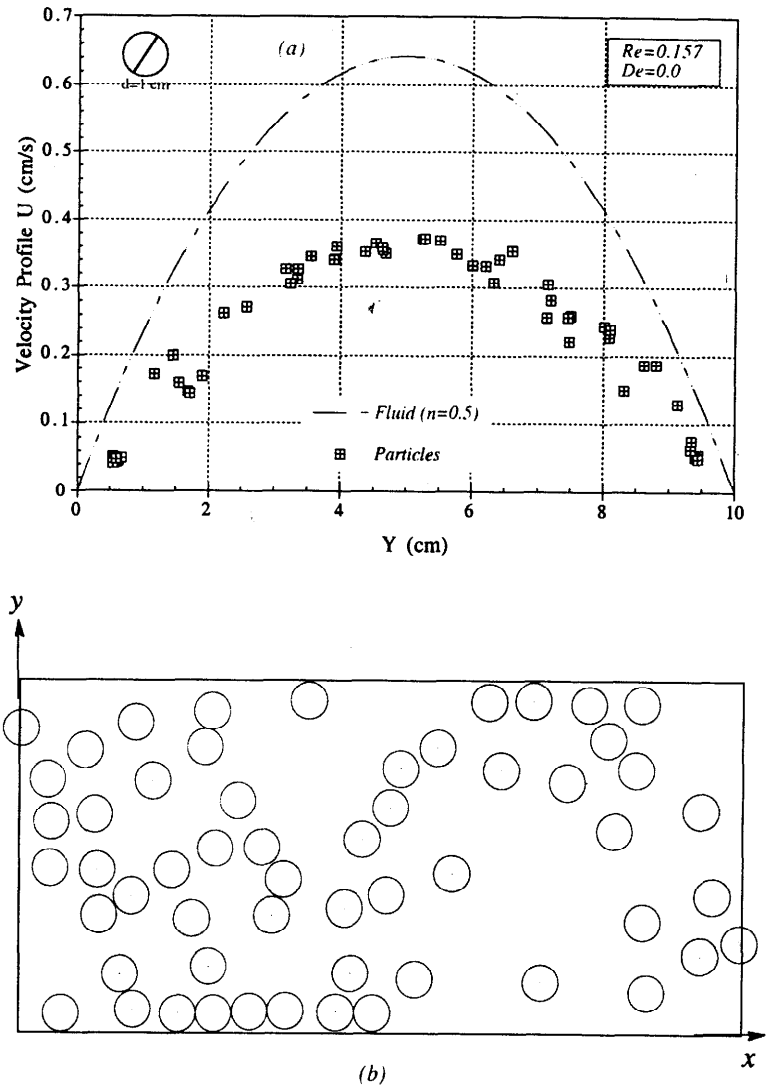

FIGURE 11. Migration of 56 neutrally buoyant particles in a pressure driven flow of a generalized Newtonian fluid (n=0.5). Re=0.157. (a) Velocity profile of the fluid without particles and the velocities of the particles; (b) particle positions in the channel at time t=3892.0 s.

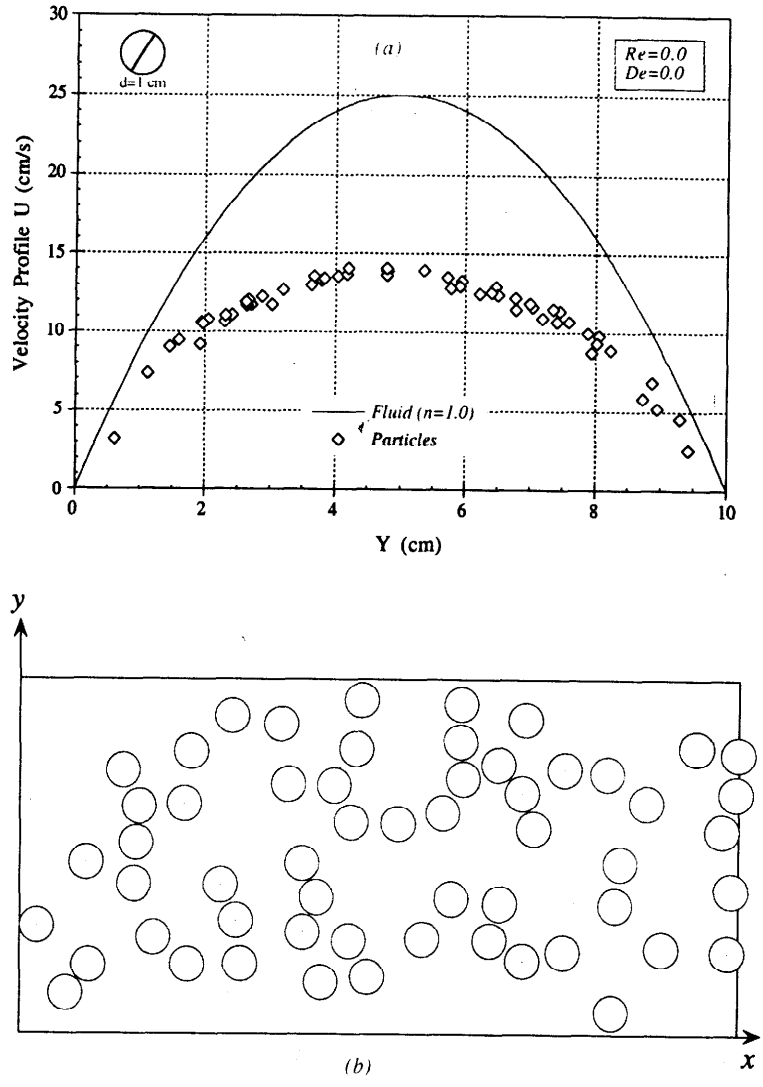

FIGURE 12. Migration of 56 neutrally buoyant particles in a pressure driven flow of a Newtonian fluid without shear thinning (n=1.0) or inertia (Re=0.0). (a) Velocity profile of the fluid without particles and the velocities of the particles; (b) particle positions in the channel at time t=43.27 s. The slip velocities at zero Reynolds number are rather large.

The flow pattern without shear thinning in figure 11 is only slightly different from that with shear thinning in figure 10. Shear thinning has very small effect when the inertia is small. To verify this, we turn off the effect of inertia completely by removing the term $\mathbf{u} \cdot \nabla \mathbf{u}$ in equation (2) so that the Reynolds number is set to zero. All the other parameters are the same as in section 4.1. The results are shown in figures 12 and 13. The flow

patterns shown in figures 10 and 12 for migrations in Newtonian fluids are quite similar to the experimental phenomenon observed by Jefri & Zahed [10] for suspensions in a pure corn syrup, which is a Newtonian fluid. In their study on migration of particles in plane-Poiseuille flow under creeping flow conditions, the neutrally buoyant particles are uniformly distributed in both the transverse and axial directions. Their particle Reynolds number is in the order of 10^{-3} and their volume fraction of solids is very low ($C_p = 0.02$).

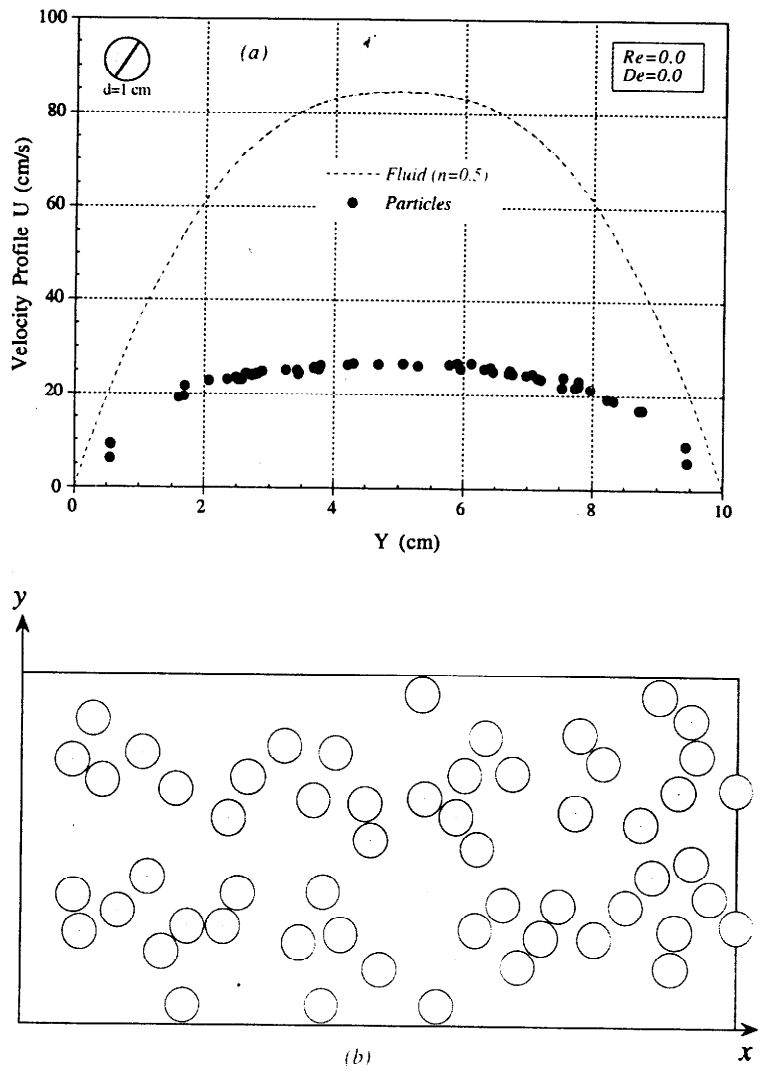

FIGURE 13. Migration of 56 neutrally buoyant particles in a pressure driven flow of a generalized Newtonian fluid (n=0.5) with no inertia (Re=0.0). (a) Velocity profile of the fluid without particles and the velocities of the particles; (b) particle positions in the channel at time t=25.42 s.

The difference in the flow patterns shown in figures 12 and 13 are relatively minor, whereas the difference in the flow patterns shown in figures 4 and 6 are considerable. In the former cases, shear thinning apparently has no effect on the particle's migration when inertia is turned off, although the difference between the slip velocities is still quite large. For flows with small inertia there is no "particle-free zone" at the centerline even if the fluid is shear thinning. Table 3 shows that there is no gap between the particles and the channel (Δ_{gap}=0.55) for n=0.5 while there is a very small gap (Δ_{gap}=0.5967) for n=1.0; this small gap could be transient.

We can conclude from figures 8-13 and table 3 that the dependence of the flow behavior on shear thinning is weak but does not vanish completely when the inertia effects are small. The weak effect of shear thinning comes from viscous stresses and is smaller when the flow is slow; in slow flow, layers of fluid without particles do not appear.

4.3. Migration in an Oldroyd-B fluid

Now consider the migration of particles in an Oldroyd-B fluid. We focus our attention on the combined effects of viscoelastic normal stresses and shear thinning after reducing the effect of inertia. First we look at the effects of viscoelasticity without shear thinning. We set parameters so that the elasticity number is above its critical value and the viscoelastic Mach number M <1; Huang, Hu and Joseph [5] have shown that in this condition the effect of elasticity is much stronger than the effect of inertia. The aforementioned condition is represented by the following particular choices of parameters: the constant viscosity of fluid $\eta = 2.0\ \mathrm{g\cdot cm^{-1}\cdot s^{-1}}$, the relaxation time $\lambda_1 = 2.0\ \mathrm{s}$ and the ratio of relaxation and retardation time $\lambda_2/\lambda_1 = 1/8$. The pressure gradient used here is the same as in figures 10 and 11: $|dp/dx| = 0.1\ \mathrm{g\cdot cm^{-2}\cdot s^{-2}}$. Then the elasticity number is fixed at E=16 throughout this section.

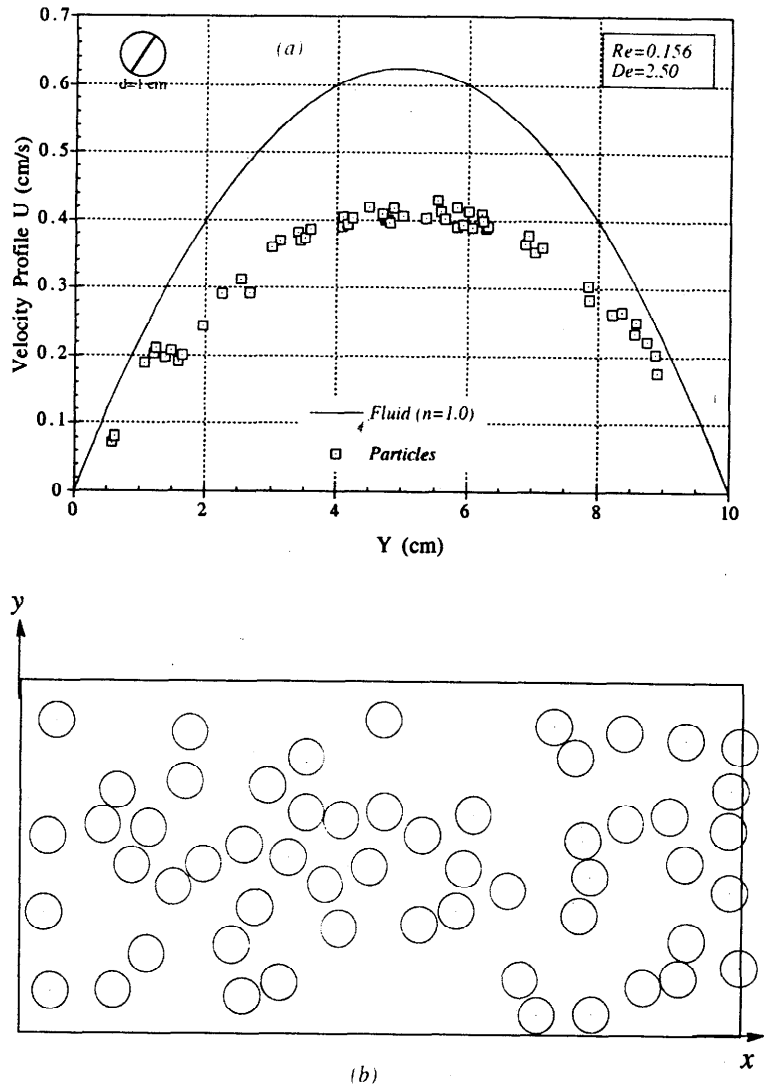

FIGURE 14. Migration of 56 neutrally buoyant particles in a pressure driven flow of an Oldroyd-B fluid without shear thinning (n=1.0). Re=0.156, De=2.50, E=16 and M=0.625. (a) Velocity profile of the fluid without particles and the velocities of the particles; (b) particle positions in the channel at time t=1613.9 s. Normal stresses associated with viscoelasticity tend to concentrate particles at the channel center.

Without shear thinning, the Reynolds number for the flow without particles is Re=0.156, the Deborah number is De=2.50 and the Mach number M=0.625. From figure 14(a) we notice that the flow pattern is very different from that in the Newtonian or generalized Newtonian fluids discussed in sections 4.1 and 4.2. There does not exist a "particle-free zone" in the centerline. Actually the particles move toward the centerline of

the channel by forces arising from viscoelastic normal stresses. The distribution of the particles at time t=1613.9 second is shown in figure 14(b). Comparing figure 14 (De=2.50) and figure 10 (De=0.0), we find that more particles migrate to the centerline for De=2.50 than for De=0.0 when all other parameters are the same.

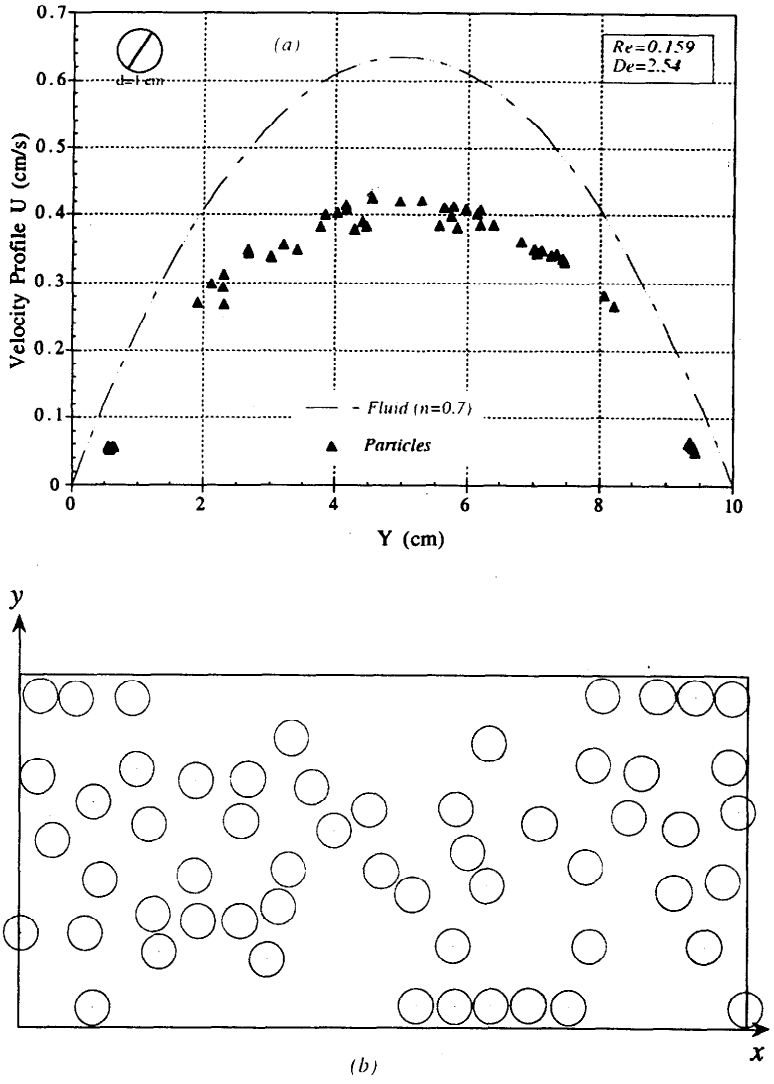

FIGURE 15. Migration of 56 neutrally buoyant particles in a pressure driven flow of an Oldroyd-B fluid with shear thinning (n=0.7). Re=0.159, De=2.54, E=16 and M=0.635. (a) Velocity profile of the fluid without particles and the velocities of the particles; (b) particle positions in the channel at time t=970.3. There are two "annular particle-free zones" and a "core particle-laden zone".

We next consider the combined effects of shear thinning and viscoelasticity. Shear thinning is inserted in the Oldroyd-B equation (3) using the Carreau-Bird expression (5) for

viscosity, with the following parameters fixed: $\eta_0 = 2.0\ \mathrm{g\cdot cm^{-1}\cdot s^{-1}}$, $\eta_\infty/\eta_0 = 0.1$ and $\lambda_3/\lambda_1 = 1.0$. All the other parameters are the same as those without shear thinning.

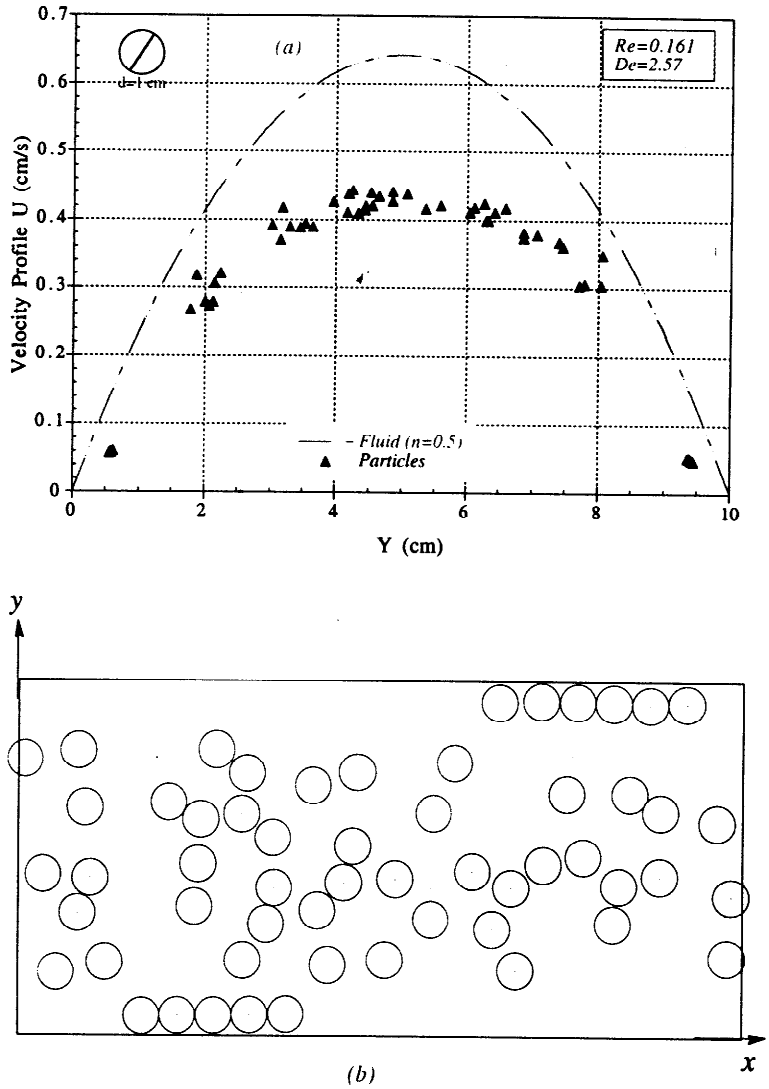

FIGURE 16. Migration of 56 neutrally buoyant particles in a pressure driven flow of an Oldroyd-B fluid with shear thinning (n=0.5). Re=0.161, De=2.57, E=16 and M=0.6427. (a) Velocity profile of the fluid without particles and the velocities of the particles; (b) particle positions in the channel at time t=1558.0.

The combination of shear thinning and viscoelasticity produces a new flow pattern; instead of creating a "particle-free zone" in the centerline as for a generalized Newtonian fluid, the elastic normal stresses move particles toward the centerline while the stresses induced by shear thinning move particles toward the channel walls, thereby creating a

"core-annular flow pattern". There are two "annular particle-free zones" and a "core particle-laden zone" in the center. Most of the particles are located in the core zone around the centerline, while others make long chains and move along the channel walls. We carry out systematic computations as shown in figures 15-17 where the power index are n=0.7, 0.5 and n=0.4, respectively.

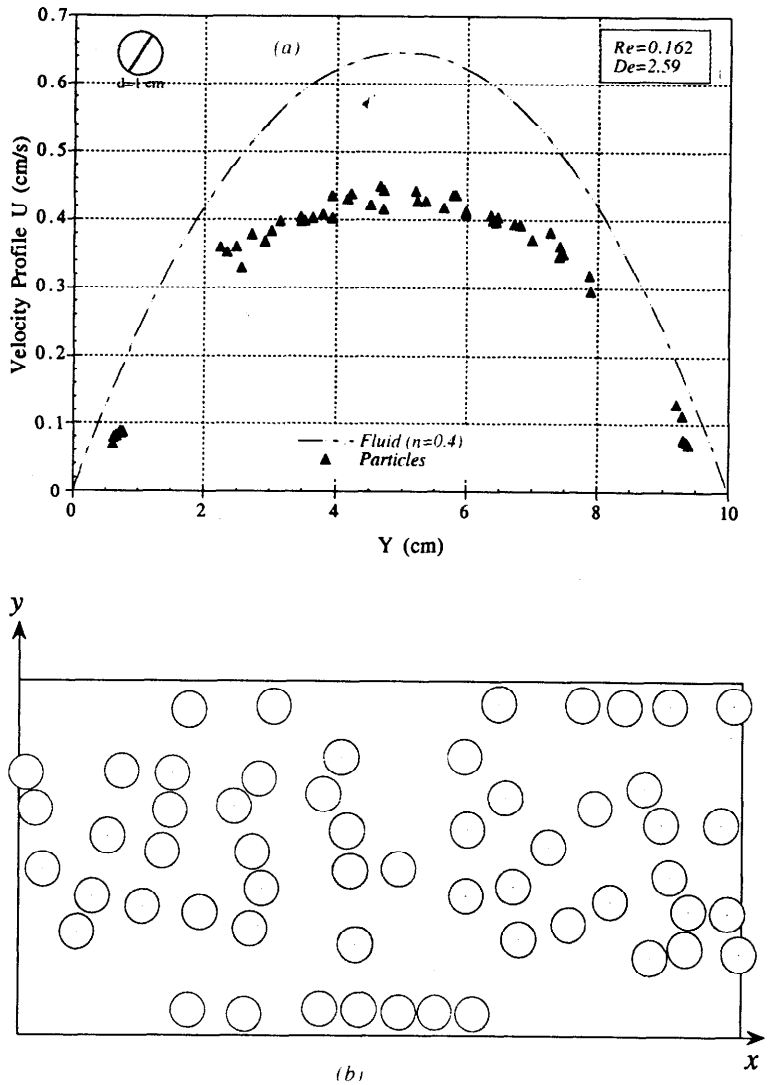

FIGURE 17. Migration of 56 neutrally buoyant particles in a pressure driven flow of an Oldroyd-B fluid with shear thinning (n=0.4). Re=0.162, De=2.59, E=16 and M=0.6466. (a) Velocity profile of the fluid without particles and the velocities of the particles; (b) particle positions in the channel at time t=1303.0.

Table 4 shows that there is no annular particle-free zone but large core particle-laden zone (Δ_{core}=8.267) when shear thinning is suppressed; the particles move everywhere but are more concentrated in the core (see figure 14) than in the Newtonian fluid shown in figure 10. The stresses induced by shear thinning when n=0.7 move the particles to the centerline, create two annular particle-free zones ($\Delta_{annular}$=1.192), and reduce the size of the particle-laden zone in the center (Δ_{core}=6.303). When the shear thinning is stronger, this phenomenon is enhanced. For n=0.5, the sizes of the annular zone and core zone are $\Delta_{annular}$=1.231 and Δ_{core}=6.286; for n=0.4, the sizes of the annular zone and core zone are $\Delta_{annular}$=1.401 and Δ_{core}=5.651.

The slip velocity does not depend strongly on the power law index, but the flows are different since inertial effects are small in these cases (Re≈0.16); the cause of the differences in the migration of particles is to be found in the combined effects of shear thinning and elasticity. The elasticity drives the particles toward the center while shear thinning moves the particles toward the channel walls.

n	Y_1	Y_2	Y_3	Y_4	$\Delta_{annular}$	Δ_{core}
1.0	0.616	——	——	8.883	——	8.267
0.7	0.644	1.912	8.215	9.330	1.192	6.303
0.5	0.614	1.784	8.070	9.362	1.231	6.286
0.4	0.760	2.242	7.893	9.212	1.401	5.651

TABLE 4. The average size of the annular particle-free zone and the size of the core zone of high particle concentration in the migration of 56 neutrally buoyant particles in a pressure driven flow of a viscoelastic fluid with shear thinning. When the effects of shear thinning increase, the size of the annular particle-free zones (Y_1, Y_2) and (Y_3, Y_4) increase while the core particle-laden zone (Y_2, Y_3) decreases. All the lengths are in centimeters.

In the experimental study by Tehrani [11], he observed the non-neutrally buoyant particles migrate toward the pipe axis in uncrosslinked and lower crosslinked fluids when the flow rate becomes high; while the particles migrate toward the pipe walls in the same fluids at low flow rate. The change of flow behavior is assumed to be the effects of

nonzero normal stresses and larger shear rate gradients. The forces, arising from both the elastic normal stresses and the shear rate gradients, drive the particles toward the region of lower shear rate at the centerline of the channel. The effects of elasticity become dominant when the flow rate becomes high, so that the fluids can be treated as viscoelastic fluids with shear thinning. The volume fraction of solids is $C_p = 0.12$.

Tehrani's experimental results are similar to our numerical computations in general but he did not mention if there are any particles near the pipe walls. This is possibly due to his experimental setup and image processing. Tehrani identified the inner wall of the pipe from images where a brighter background lighting was used. The presence of the particles were recognized by scanning the intensity profiles from left to right. If there were peaks with intensities less than 60%-70% of the average value, then these values were discounted. In that way, the low concentration of particles near the walls may be either out of the inner walls or discounted, so he observed only the "core particle-laden zone" but no "annular particle-free zone".

In high crosslinked fluids, Tehrani found that the particles migrate toward the pipe center even if the flow rates are low. When the fluids are higher crosslinked, particles migrate at the beginning and soon form a roughly uniform distribution near the central region. Tehrani believed that shearing at this central plug becomes very small because of the presence of the high concentration of the solids, resulting in a high viscosity. Without high shear rate gradients, the particles no longer migrate, even with the high normal stresses. The flow conditions in Tehrani's experiments were chosen to be similar to hydraulic fracturing operations, having the particle Reynolds number of order 10^{-4}~1 and Deborah number in the order of 50.

On the other hand, Jefri & Zahed [10] found that neutrally buoyant particles tend to migrate toward the centerline, creating a narrow core in a non-shear thinning elastic medium, the same phenomenon as in our computation results. However, Jefri & Zahed [10] also found that the particles migrate to an annular region between the walls and the

centerline of the channel in a shear thinning elastic fluid. They did not comment on this flow behavior. The flow rate in their experiments is very slow so that the effect of inertia is negligible ($\mathrm{Re} \propto 10^{-4}$), their volume fraction of solids is very low ($C_p = 0.02$) but the effect of elasticity is extremely high ($De \propto 10^2$). The flow behavior observed by Jefri & Zahed [10] is different than that observed by Tehrani [11], but the source of this difference is not shown. Our simulations do not rise to the experiments because they do not converge for De>5.

4.4. Effect of volume fraction of solids

To study the effect of volume fraction of solids on flow behavior, we double the number of particles from 56 to 112 in the channel and consider Newtonian, generalized Newtonian and shear thinning Oldroyd-B fluids. The volume fraction of 112 particles in our flow domain is $C_p = 0.42$. Figures 18 and 19 show that "particle-free zones" at the channel center in Newtonian and generalized Newtonian fluids are suppressed in concentrated dispersions. The channel center is basically shear free; the migration away from the center in more dilute cases is caused by the curvature of the velocity profile.

The main effect of the increased loading of solids is to suppress the migration of particles away from the center where the effects of shear thinning are the weakest because the shear rates are small (cf. figures 4 and 18 for Re=12.5 and n=10, and figures 6 and 19 for Re=42.3 and n=0.5). This migration away from the center is generally believed to be an effect of the curvature of the velocity profile (see Asmolov [14]), an effect which may be diminished by the presence of many particles. With high volume fraction of solids, the effects of slip velocity have been greatly reduced. As can be seen in table 5, the slip velocities are even higher with high C_p because the particles move much slower. Instead of migrating toward the channel walls, the particles now stay near the center region with almost no migration, as shown in figures 18 and 19. On the other hand, the effects of shear thinning at the walls are not so strongly changed by the increase in the volume fraction of solids.

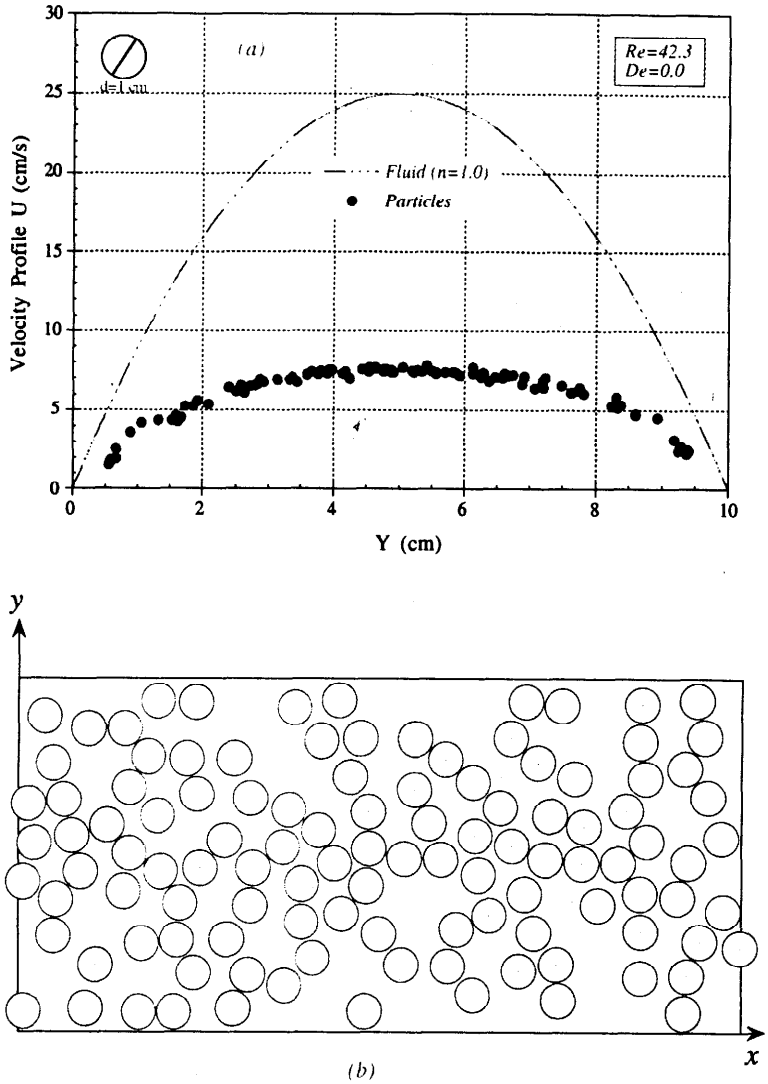

FIGURE 18. Migration of 112 neutrally buoyant particles in a pressure driven flow of a Newtonian fluid (n=1.0). Re=12.5. (a) Velocity profile of the fluid without particles and the velocities of the particles; (b) particle positions in the channel at time t=71.66 s.

C_p	n	Re	U_{max}	U_p	U_{slip}
0.21	1.0	12.5	25	15	10
0.42	1.0	12.5	25	7.8	17
0.21	0.5	42.3	84.5	29.6	54
0.42	0.5	42.3	84.5	23.8	61

TABLE 5. The maximum slip velocity of the neutrally buoyant particles. U_{slip} increases when the volume fraction of solids C_p becomes larger.

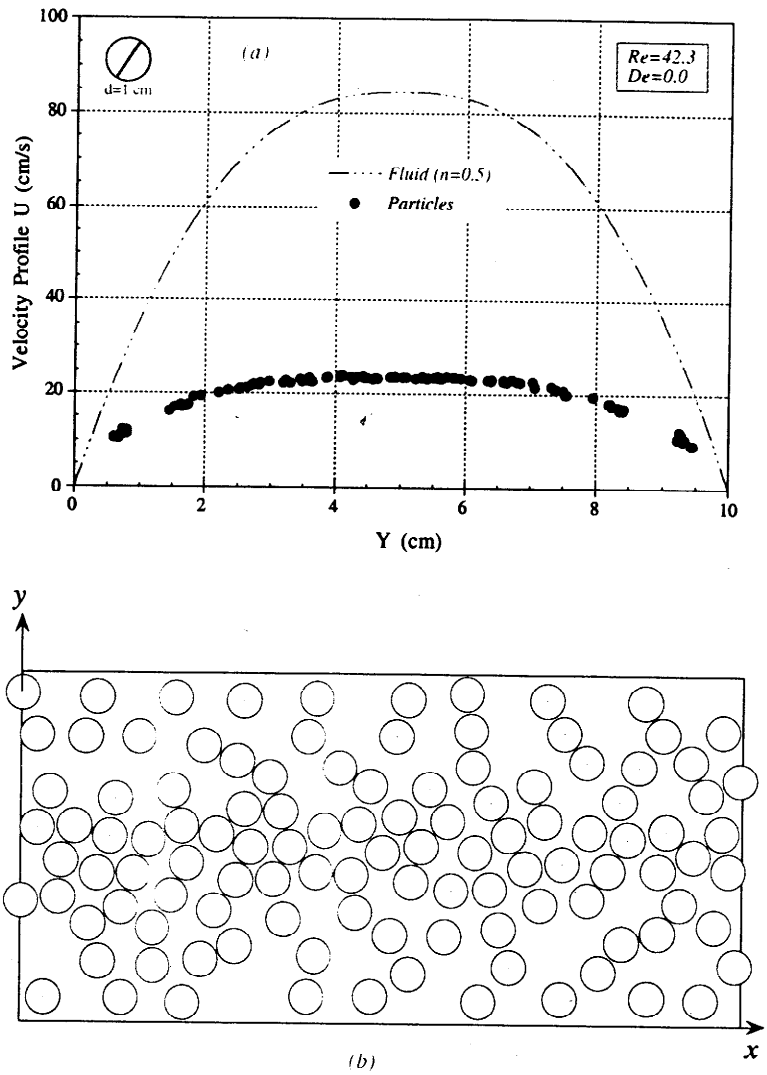

FIGURE 19. Migration of 112 neutrally buoyant particles in a pressure driven flow of a generalized Newtonian fluid (n=0.5). Re=42.3. (a) Velocity profile of the fluid without particles and the velocities of the particles; (b) particle positions in the channel at time t=42.67 s.

In an Oldroyd-B fluid (Re=0.161, De=2.57, E=16, M=0.6427 and n=0.5), as can be seen in figure 20, the flow pattern shows no significant difference from the more dilute case in figure 16 although the annular "particle-free zone" is smaller due to the high volume fraction. The effect of elasticity moves the particles toward the centerline, while shear thinning moves particles toward the channel walls, creating a small annular "particle-free zone". The high volume fraction decreases the shear rate, thus decreasing the effects of

both shear thinning and elastic normal stresses. It is particularly noteworthy that the combined effect of shear thinning and elasticity leads to chains of particles on the wall for both high and low solids loadings.

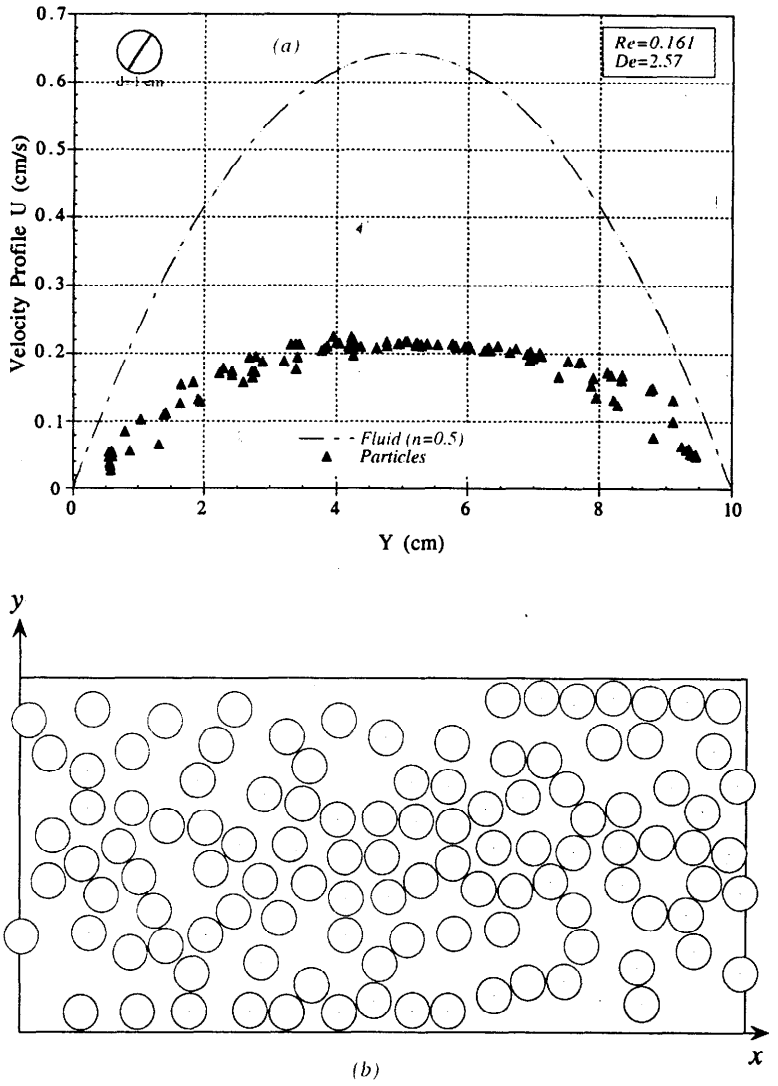

FIGURE 20. Migration of 112 neutrally buoyant particles in a pressure driven flow of an Oldroyd-B fluid with shear thinning (n=0.5). Re=0.161, De=2.57, E=16, M=0.6427. (a) Velocity profile of the fluid without particles and the velocities of the particles; (b) particle positions in the channel at time t=1594 s.

Tehrani [11] also studied the effect of solids concentration. He found that the rate of migration toward pipe axis in high degree of crosslinking fluids decreases rapidly once the centerline concentration reaches around 0.3. As the concentration near the axis increases,

the shear rate at the region near the centerline decreases, resulting in the increasing of the viscosity. When viscosity increases, the driving force for migration toward the centerline, arising from the local normal stresses and the shear rate gradient, decreases; while the resisting force arising from viscosity increases.

5. Conclusions

The flow behavior of neutrally buoyant particles migrating in a pressure driven flow of Newtonian and viscoelastic fluids, depends strongly on the volume fraction of solids, the blockage ratio of the channel, the effects of inertia and elasticity, and the effects of shear thinning.

Inertia always tends to move particles away from the channel walls and from the centerline of the channel, while the elasticity causes them to migrate toward the centerline.

In general, shear thinning moves the particles away from the centerline but toward the channel walls when the inertia or elasticity is strong enough.

In Newtonian or generalized Newtonian fluids at moderate Reynolds numbers, when the effects of shear thinning become stronger, the particle-free zone along the centerline of the channel becomes larger and the particles move closer to the channel walls, as long as the effect of inertia is strong enough. If the effect of inertia is too weak, the dependence of the flow behavior of the particles on the shear thinning is very weak.

The effects of shear thinning and the curvature of the velocity profile induce strong shear stresses and large slip velocities, thus causing the particles to migrate away from the centerline of the channel and move toward the channel walls.

In a viscoelastic fluid, the particles migrate toward the centerline of the channel even without shear thinning. With shear thinning, most of the particles migrate toward a core zone in the center of the channel, while others form long chains and move along the channel walls. There exist two "annular particle-free zones" and a "core particle-laden zone". The core zone becomes narrower as the effect of shear thinning is increased.

A high volume fraction of solids prevents the formation of the particle-free zone at the centerline of the channel in Newtonian and generalized Newtonian fluids since the shear rate becomes very small, although the slip velocity becomes larger. The volume fraction of solids has a weaker effect on the migration in a viscoelastic fluid, it decreases the size of the annular particle-free zone.

Acknowledgment: This work was partially supported by National Science Foundation Grand Challenge grant KDI (NSF/CTS-98-73236), by the US Army, Mathematics, by the DOE, Department of Basic Energy Sciences, by a grand from the Schlumberger foundation, and from Stimlab Inc. and by the Minnesota Supercomputer Institute.

References

[1] D. V. Boger, Demonstration of upper and lower Newtonian fluid behavior in a pseudoplastic fluid. Nature, 265 (1977) 126-127.

[2] D. D. Joseph, Flow induced microstructure in Newtonian and viscoelastic fluids. In Proc. of 5th World Congress of Chem. Engng., Particle Technology Track, San Diego. July 14-18. AIChE , 6 (1996) 3-16.

[3] P. Y. Huang, J. Feng, H. H. Hu & D. D. Joseph, Direct simulation of the motion of solid particles in Couette and Poiseuille flows of viscoelastic fluids. J. Fluid Mech. 343 (1997) 73-94.

[4] S. H. Garrioch & D. F. James, A finite-element study of Newtonian and power-law fluids in conical channel flow. J. Fluids Engng., 119 (1997) 341-346.

[5] P. Y. Huang, H. H. Hu & D. D. Joseph, Direct simulation of the motion of elliptic particles in Oldroyd-B fluids. J. Fluid Mech., 362 (1998) 297-325.

[6] J. F. Morris & J. F. Brady, Pressure-driven flow of a suspension: Buoyancy effects. Int. J.. Multiphase Flow, 24 (1998) 105-130.

[7] G. Segré & A. Silberberg, Radial particle displacements in Poiseuille flow of suspensions. Nature, 189 (1961) 209-210.

[8] A. Karnis & S. G. Mason, Particle motions in sheared suspensions. XIX. Viscoelastic media. Thans. Soc. Rheol., 10 (1966) 571-592.

[9] F. Gauthier, H. L. Goldsmith & S. G. Mason, Particle motions in non-Newtonian media II. Poiseuille flow. Thans. Soc. Rheol., 15 (1971) 297-330.

[10] M. A. Jefri & A. H. Zahed, Elastic and viscous effects on particle migration in plane-Poiseuille flow. J. Rheol., 33 (1989) 691-708.

[11] M. A. Tehrani, An experimental study of particle migration in pipe flow of viscoelastic fluids. J. Rheol., 40 (1996) 1057-1077.

[12] H. Binous & R. J. Phillips, Dynamic simulation of one and two particles sedimenting in a viscoelastic suspension of FENE Dumbbells. J. Non-Newtonian Fluid Mech., (1998) (submitted).

[13] H. Binous & R. J. Phillips, The effect of sphere-wall interactions on particle motion in a viscoelastic suspension of FENE Dumbbells. J. Non-Newtonian Fluid Mech., (1998) (submitted).

[14] E. S. Asmolov, The inertial lift on a spherical particle in a plane Poiseuille flow at large channel Reynolds number. J. Fluids Engng., 381 (1999) 63-87.